Journal of Biomolecular Structure and Dynamics

ISSN: 0739-1102 (Print) 1538-0254 (Online) Journal homepage: www.tandfonline.com/journals/tbsd20

Biochemical and biophysical characterization of biosynthetic arginine decarboxylase from *Thermus thermophilus*

Veerapandiyan Malaisamy, Karthika Alagesan, Hemavathy Nagarajan, Manikandan Jayaraman, Umashankar Vetrivel & Jeyakanthan Jeyaraman

To cite this article: Veerapandiyan Malaisamy, Karthika Alagesan, Hemavathy Nagarajan, Manikandan Jayaraman, Umashankar Vetrivel & Jeyakanthan Jeyaraman (2025) Biochemical and biophysical characterization of biosynthetic arginine decarboxylase from *Thermus thermophilus*, Journal of Biomolecular Structure and Dynamics, 43:12, 5917-5934, DOI: 10.1080/07391102.2024.2314753

To link to this article: https://doi.org/10.1080/07391102.2024.2314753

JOURNAL OF BIOMOLECULAR STRUCTURE AND DYNAMICS
2025, VOL. 43, NO. 12, 5917–5934
https://doi.org/10.1080/07391102.2024.2314753

Biochemical and biophysical characterization of biosynthetic arginine decarboxylase from *Thermus thermophilus*

Veerapandiyan Malaisamy[a], Karthika Alagesan[a], Hemavathy Nagarajan[a,b], Manikandan Jayaraman[a], Umashankar Vetrivel[c] and Jeyakanthan Jeyaraman[a]

[a]Structural Biology and Bio-Computing Lab, Department of Bioinformatics, Science Block, Alagappa University, Karaikudi, Tamil Nadu, India; [b]Centre for Bioinformatics, Vision Research Foundation, Chennai, Tamil Nadu, India; [c]ICMR-Department of Virology and Biotechnology/ Bioinformatics Division, National Institute for Research in Tuberculosis, Chennai, Tamil Nadu, India

ABSTRACT

The biosynthetic arginine decarboxylase in *Thermus thermophilus* is responsible for producing spermidine, a polyamine with numerous biological applications in humans. The arginine decarboxylase has significant applications in biotechnology industries, suggesting the need to evaluate its biochemical and biophysical characteristics at the molecular level. In this study, both *in vitro* and *in silico* methods were employed to investigate the structural and functional behavior of the arginine decarboxylase protein. In *in vitro,* MALDI-TOF, size exclusion, and assay studies were performed to examine the nature and activity of the protein. The MALDI-TOF analysis confirmed the purified protein as biosynthetic arginine decarboxylase. The assay results revealed that the Pyridoxal 5′-Phosphate (PLP) cofactor plays a crucial role in enhancing enzyme activity by producing agmatine (a by-product of spermidine). Further, optimum enzyme activity was observed at 50 °C, suggesting the extremophilic nature of the enzyme. Unlike other proteins, this enzyme displayed optimal activity at both acidic and basic pH, demonstrating its sensitivity to pH changes. Furthermore, the addition of divalent ions like Mg^{2+} increased the rate of reaction. In *in silico*, structure modeling, and comparative molecular dynamics simulation studies were used to assess the protein stability and behavior at different pH and temperature conditions. The findings of this study could be applied to improve enzyme production in the industry.

ARTICLE HISTORY
Received 16 June 2023
Accepted 29 January 2024

KEYWORDS
Thermus thermophilus; biosynthetic arginine decarboxylase; MALDI-TOF; Activity assay; molecular dynamics simulation

1. Introduction

Thermus spp. are widespread thermophilic bacteria found in both natural and manmade thermal environments (Cava et al., 2009). In systems biology, *T. thermophilus* (HB8) is one of the model organisms (Ohtani et al., 2010). This bacterium is gram-negative, rod-shaped, non-motile, and non-sporulating (Tabor & Tabor, 1984; Teh et al., 2012). *T. thermophilus* (HB8) is an extremophile capable of surviving in extreme conditions, such as high temperatures, pressure, salinity, alkalinity, and acidity. This aerophilic bacterium was isolated from thermal vents in Izu-Japan and can grow at temperatures ranging from 50°C to 85°C (Hori, 2019). These organisms produce a variety of biologically and industrially important extremozymes that enable them to survive in such extreme environmental conditions (Arora et al., 2022).

T. thermophilus is capable of producing 16 types of rare cellular polyamines; hence it is considered the powerhouse of polyamines (Kobayashi et al., 2022; Ohtani et al., 2010). Polyamines are small polycationic molecules that serve a range of biological functions (Takahashi & Kakehi, 2010). Putrescine, spermidine, and spermine are the three standard linear polyamines produced by most living organisms (Tabor & Tabor, 1985). In addition to these standard polyamines, *T. thermophilus* can also produce long-chain polyamines like caldopentamine and caldohexamine, as well as branched-chain polyamines like tetrakis (3-aminopropyl) ammonium (Terui et al., 2005). These polyamines play an essential role in regulating cell growth by withstanding high temperatures. The long linear polyamine was reported to play a crucial role in stabilizing DNA, whereas the branched polyamine was found to stabilize RNAs of *T. thermophilus* (Bae et al., 2018). In addition, *in vitro* reports also revealed the essentiality of quaternary amines for polypeptide biosynthesis. These polyamines stabilize the complex between ribosomes, the mRNA, and phenylalanyl-tRNA, which aids in protein production (Uzawa et al., 1993). Polyamines also play a crucial role in nucleic acid stabilization, translation, and regulating both oxidative salt, and temperature stress conditions (Gevrekci, 2017). Spermidine, a natural polyamine found in various organisms, is a geroprotector that prolongs the lifespan of fungi, nematodes, insects, and rodents. As well as decreasing

CONTACT Jeyakanthan Jeyaraman jjbioinformatics@gmail.com Structural Biology and Bio-Computing Lab, Department of Bioinformatics, Science Block, Alagappa University, Karaikudi, 630 003, Tamil Nadu, India

Supplemental data for this article can be accessed online at https://doi.org/10.1080/07391102.2024.2314753.

the onset of cardiovascular disease and neurodegeneration diseases in mice, it also prevents various age-associated diseases (Hofer et al., 2022). In specific, spermidine inhibits tumor cell proliferation and suppresses tumor growth by interfering with its cell cycle (Prasher et al., 2023).

In *T. thermophilus*, the proteins *Spe*A, B, D, and E are involved in the production of polyamines (Tairo Oshima, 2010). The *Spe*A gene encodes arginine decarboxylase, *Spe*B encodes agmatine ureohydrolase, *Spe*D encodes SAM decarboxylase, and *Spe*E encodes either spermidine synthase or spermine synthase (T. Oshima, 2007). The polyamines in *T. thermophilus* are synthesized from L-arginine, which is converted to agmatine by arginine decarboxylase, requiring both Pyridoxal 5′-Phosphate (PLP) and Mg^{2+} as cofactors (Figure 1). Wherein, agmatine acts as a precursor for spermidine production (Tabor & Tabor, 1985). Recent studies on agmatine biosynthesis in mammals have renowned interest in its potential therapeutic applications. Agmatine has exceptional modulatory effects on molecular targets, including neurotransmitter systems, nitric oxide synthesis, and polyamine metabolism, leading to increased recognition in the pharmaceutical industry (Sun et al., 2017). Not only the end product but also the by-product in this pathway has great importance. Hence in the present study, we have examined the activity of *Spe*A using both *in vitro* and *in silico* methods, as well as the effects of pH, temperature, and ions on protein function were analyzed.

2. Methodology

2.1. Cloning and expression of T. thermophilus biosynthetic arginine decarboxylase

The biosynthetic arginine decarboxylase, encoding the *Spe*A gene (Gene ID: 3169310), was PCR amplified from the *T. thermophilus* HB8 genomic DNA (Henne et al., 2004). The amplified product was cloned into the pET11a (Novagen) expression vector. The cloned pET11a vector containing the *Spe*A gene was then transformed into an *Escherichia coli* BL21 (DE3) expression system. The primary cultures were grown overnight at 37°C in a sterile medium containing 100 mg/mL ampicillin. The primary culture was then transferred to four liters of Luria Bertani broth and grown until A600 reached an OD of 0.6-0.8. Expression of the protein was induced by adding Isopropyl β-d-1-thiogalactopyranoside (IPTG) and incubated for 5 hr.

2.2. Purification of recombinant protein

The grown cells were harvested and resuspended in the buffer containing 30 mM Sodium Phosphate ($NaHPO_4$), 30 mM Sodium chloride (NaCl), 3% Beta mercaptoethanol (βME), 1 mM Phenylmethylsulfonyl fluoride (PMSF), and 1 mM Dithiothreitol (DTT). The cells were sonicated for 15 min at 55 amp with a 7-pulse on and 9-pulse off. The sonicated lysate was centrifuged at 10,000 rpm and the supernatant was taken and kept in a water bath for 20 min at 70°C. The *Thermus* biosynthetic arginine decarboxylase will remain intact while other heat-labile proteins will be denatured (Tamakoshi & Oshima, 2011). The denatured proteins were removed by centrifugation at 10,000 rpm for 20 min. The supernatant-containing protein was loaded into the HiTrap QFF column (GE Healthcare). The column was pre-equilibrated with buffer A and the protein was eluted by stepwise gradient using buffer A (30 mM $NaHPO_4$, 30 mM NaCl, 3% βME) and buffer B (30 mM $NaHPO_4$, 1 M NaCl, 3% βME). Further, Gel Filtration Chromatography - SEC-HiLoad ® 16/600 Superdex ® 200 pg (GE Healthcare) was used for the purification of the protein, using 30 mM $NaHPO_4$, 30 mM NaCl buffer. Bovine Serum Albumin (Sigma Aldrich) was used as a standard for Gel Filtration Chromatography. The purity of the protein was checked using 12% Sodium dodecyl sulfate- Polyacrylamide gel electrophoresis (SDS-PAGE).

2.3. MALDI-TOF/TOF analysis

MALDI-TOF/TOF analysis was performed to confirm whether the purified protein is a biosynthetic arginine decarboxylase or not. The band containing the targeted protein was excised from SDS-PAGE by chopping it into small pieces followed by destaining. A solution of 50% acetonitrile (ACN) and 25 mM ammonium bicarbonate (NH_4HCO_3) was used and incubated at room temperature for 10 min; the procedure was repeated until the gel was completely destained. About 10 mM DTT and 100 mM ammonium bicarbonate were added, and the mixture was incubated at room temperature for 15 min. The solution was centrifuged, and the supernatant was discarded. The pellet was alkylated by treating it with 50 mM iodoacetamide, which was dissolved in 100 mM NH_4HCO_3. Trypsin digestion was performed by adding 20 μL of trypsin and incubating it for 16 hr. The 5% TriFluoro acetic acid (TFA) and 50% ACN were added to it and centrifuged. The supernatant-containing peptides were considered for MALDI TOF/TOF analysis. The peptide mass was analyzed using the Proteomics Facility, Indian Institute of Science

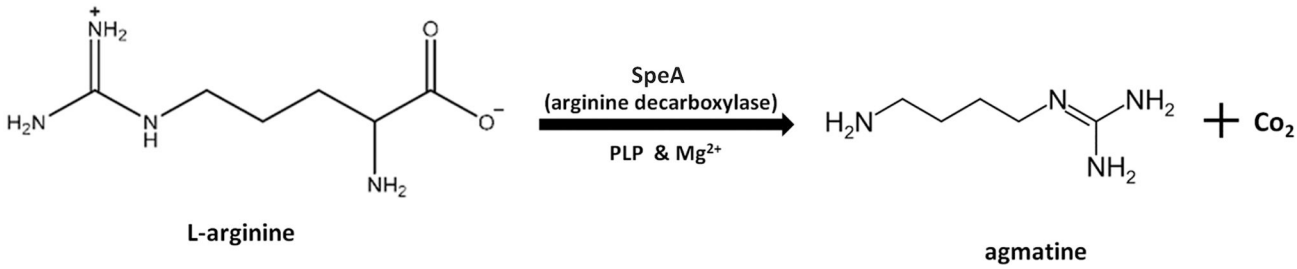

Figure 1. Mechanism for the formation of agmatine by arginine decarboxylase.

(IISc), Bangalore using Bruker Daltonics GmbH's UltrafleXtreme MALDI TOF/TOF instrument, Bremen, Germany. The 10 mg/ml of CHCA (α-cyano-4-hydroxy transcinnamic acid) was used as a matrix. The MALDI-TOF/TOF fitted with a 337 nm nitrogen laser was used to measure charged ions (Murray et al., 2016). Further, the peptide mass fingerprint was analyzed using the MASCOT against the UP279841_*T.thermophilus* database. Since the taxonomy of *T.thermophilus* is not there on the MASCOT page, other bacteria were chosen as the organism source. Carbamidomethylation of cysteine and oxidation were selected for variable modification, whereas one maximum missing cleavage was set, and the mass tolerance of 200 ppm per peptide was fixed and analyzed (Joyner et al., 2013; Thiede et al., 2005).

2.4. Prediction of tertiary structure of biosynthetic arginine decarboxylase

The amino acid sequences of biosynthetic arginine decarboxylase encoded by the *Spe*A gene were retrieved from the UniProtKB database (UniProt ID: Q5SHU0) ("The Universal Protein Resource (UniProt)", 2007). The three-dimensional (3D) structure of biosynthetic arginine decarboxylase is a prime requisite to evaluate its structure and function. The amino acid sequence of biosynthetic arginine decarboxylase was analyzed in BlastP (Altschul et al., 1990) against the protein data bank (PDB) database to detect the most suitable templates for building the 3D structure. Subsequently, homology modelling of biosynthetic arginine decarboxylase was carried out using MODELLER version10 based on the alignment between the target and template protein sequences (Webb & Sali, 2016). The predicted model was structurally validated using the SAVES server v6.0. The ERRAT (Colovos & Yeates, 1993) and Verify3D (Eisenberg et al., 1997) were considered as parameters for assessing the physicochemical properties to verify the modelled structure. Finally, ProSA (Protein Structure Analysis) (Wiederstein & Sippl, 2007) with default parameters was used to examine the overall quality of the modelled structure by calculating the Z-score value.

2.5. Activity assay

The activity of biosynthetic arginine decarboxylase was estimated by following the protocol reported previously (Alam et al., 2018). The assay was performed with the buffer containing 30 mM $NaHPO_4$, 30 mM NaCl, 1.5 mM DTT, and 40 mM PLP. A concentration of 1 mM of protein (enzyme) and 25 mM of substrate L-arginine was added to initiate the reaction and incubated at 37°C. The reaction was stopped by adding potassium hydroxide (KOH) which was saturated with NaCl. In order to separate the produced agmatine, n-butanol was added and vortexed for a minute. Further, it was centrifuged, and the butanol layer containing agmatine was extracted and mixed with the diacetyl reagent (Alam et al., 2018). If agmatine is present upon the addition of diacetyl reagent it will form a red color that was measured at 530 nm using a spectrophotometer. The blank containing all other components without enzymes and a blank without substrates were used as controls. In order to determine the actual enzymatic reaction rate, we subtract the control date (non-enzyme blank) from the experimental data. The optimum activity of arginine decarboxylase was examined with and without the presence of substrate and cofactor and by differing the time of incubation (0 min – 1 hr). Also, the effect of pH (4-11), temperature (20°C –90°C), and different metal ions such as Mg^{2+}, Cu^{2+}, Mn^{2+}, and Ni^{2+} on agmatine formation were examined. In the pH-dependent assay, the effect of pH on agmatine formation was observed using a constant buffer and by varying the buffer system. In the case of a constant buffer, 30 mM Sodium Phosphate buffer ($NaHPO_4$), 30 mM NaCl, 1.5 mM DTT, and 40 mM PLP were used to analyze the activity of the protein at all pH levels (4 to 11). For different buffer systems, the activity was analyzed by replacing the 30 mM Sodium Phosphate ($NaHPO_4$) with other buffers as follows: Citrate buffer was used for pH 4-6, Tris-HCl buffer for pH 7-9, Glycine-sodium hydroxide (NaOH) buffer for pH 10, and a Sodium bicarbonate ($NaHCO_3$)-Sodium hydroxide (NaOH) buffer for pH 11. All experiments were conducted in biological and experimental triplicates, and all statistical analyses were calculated using GraphPad Prism software 9.0.

2.6. Effect of pH, and temperature on structural changes of biosynthetic arginine decarboxylase

The Mg^{2+} ion and PLP cofactor were found to be essential in the functioning of biosynthetic arginine decarboxylase (Alam et al., 2018; Wu et al., 2015). Therefore, the 3D structure of biosynthetic arginine decarboxylase was reconstructed with Mg^{2+} ion based on the crystal structure of human ornithine decarboxylase (PDB ID: 4ZGY). Molecular dynamics simulation (MDS) is a comprehensive computational approach used to study various biomolecular events such as conformational change, ligand binding, and protein folding (Hollingsworth & Dror, 2018). MD of protein-ligand complex interactions may offer exact information on a protein's dynamic movement (Shukla & Tripathi 2020). The use of MD simulations to simulate the behavior of proteins at different pHs and temperatures will provide insight into the stability determinants of proteins (Boroujeni et al., 2021). Initially, the modelled and refined *apo* biosynthetic arginine decarboxylase was subjected to MD to determine its structural stability. Subsequently, using PLP as a cofactor, the MD simulation study was carried out under a variety of pH environments (acidic: pH 5, neutral: pH 7, and alkaline: pH 8 and pH 11) and temperature settings (300K, 323.15K, 353.15K, and 363.15K). Further, the conformational dynamics of biosynthetic arginine decarboxylase with its substrate (L-arginine) were also investigated using Desmond. The OPLS-2005 force field was used to inspect the stability of *apo* and complexes. The *apo* and *holo* forms of the protein were prepared with a system builder platform and were solvated using the simple point charge (SPC) explicit water model. The distance between the protein surface and the edge of the box was set at 10 Å. The appropriate number of counter ions (Na^+ or

Cl^-) were added to neutralize the system only for the pH 7 condition. Two rounds of equilibrations were performed, starting with an NVT ensemble, followed by an NPT ensemble for each interval of 100 ps for the relaxation of systems before simulation. To calculate long-range electrostatic interactions, the particle mesh Ewald (PME) technique (Kawata & Nagashima, 2001) was applied with the radius for Coulomb interactions set at 9 Å. Finally, the equilibrated systems were subjected to production dynamics for a 200 ns time scale. The structural stability indicator parameters, root mean square deviation (RMSD), and root mean square fluctuation (RMSF) were calculated to ensure structural stability, and residual flexibility, respectively.

2.7. Molecular docking and MM/GBSA binding energy calculation

The molecular interaction study (covalent docking) between the binding site residues of biosynthetic arginine decarboxylase and the PLP cofactor was performed with the aid of CovDock of the Schrödinger suite (Schrödinger, LLC, New York, United States). Further, the binding energy calculation based on the MM-GBSA approach was implemented with the prime module of the Schrödinger suite to calculate the binding affinity between the protein and cofactor in the complexes by employing the VSGB solvation model (Li et al., 2011) and OPLS4 force field.

3. Results and discussion

3.1. Expression and purification of recombinant protein

The Recombinant biosynthetic arginine decarboxylase from *T. thermophilus* HB8 protein was cloned into a bacterial expression vector. Further, the protein was overexpressed with IPTG induction of 0.7 mM. The overexpressed protein was further subjected to ion exchange chromatography, resulting in 80% purity of the protein. Further, to obtain pure protein, size exclusion chromatography was performed, and highly pure protein was obtained with the single band on SDS-PAGE (Figure 2a). In size exclusion, the protein eluted just before the standard BSA elution, and only one peak was observed. The size exclusion results show that in the solution state, the protein was observed to be a monomer. Using SDS-PAGE, the molecular mass of the protein was estimated to be ~70 kDa, which correlates with the theoretical estimated value of 70,241 Da (Figure 2b). As the crystal structure of arginine decarboxylase from *T. thermophilus* is not available, a homology model was prepared using the crystal structure of arginine decarboxylase from *E.coli* (PDB ID: 3NZQ) as a template (Forouhar et al., 2010). This template was found to be highly suitable as it had a high sequence identity score of 40.5%, query coverage of 97%, and a lower e-value of 3e-160. Among the 100 models generated, the model having the high negative discrete optimized potential energy (DOPE) score was taken for validation. The modelled structure had an acceptable ERRAT quality score of 80.1%, a VERIFY 3D score of 95.2%, and no PROCHECK errors. The reliability of the predicted model structure was then established with a maximum amino acid percentage in the favored and allowed regions of the Ramachandran plot (Figure 1). Moreover, the obtained ProSA Z score of −11.41 indicated the overall model quality of biosynthetic arginine decarboxylase. The results of several structural evaluation methods suggested that the predicted model has fewer unfavorable conformations and improved model quality. In addition, the available AlphaFold model (ID: AF-Q5SHU0-F1) was compared with the homology modelled structure, and it was observed to have RMSD deviation of 1.317 Å, which depicts the similarity of conformation. Based on the information acquired from 4ZGY, the Mg^{2+} ion was positioned appropriately in the validated model of biosynthetic arginine decarboxylase (Figure 3) (Wu et al., 2015).

3.2. Molecular dynamics simulation of apo biosynthetic arginine decarboxylase protein

The stability of the modelled biosynthetic arginine decarboxylase was structurally verified by MD simulation at room temperature (300 K) for a period of 200 ns. The computed structural stability indicators, such as RMSD and RMSF, are shown in Figure 4. The backbone RMSD plot established a well-maintained equilibrium pattern throughout the simulation run with an RMSD value below ~10Å (Figure 4a). The RMSF profile forecasted the flexible residues in the biosynthetic arginine decarboxylase structure by displaying high flexible peaks in the plot (Figure 4b). Two regions showed high flexible peaks in the plot, F1 and F2, corresponding to residues from Ala362-Arg418 and Ala588-Asp628, respectively. Additionally, the predicted model of biosynthetic arginine decarboxylase protein was energetically stable during the simulation (Figure 4c), as shown by the minimum potential energy. The residues from Ala362-Arg418 and Ala588-Asp628 show considerable structural displacement, as observed when the initial and energetically minimized structures were superimposed (Figure 4d). These regions also display significant flexible peaks on the RMSF plot.

3.3. Identification of purified protein using MALDI_TOF/TOF

In the MALDI results, the monoisotopic peaks were observed in the range of m/z ratio of 600-3000 kDa. The obtained MALDI-TOF/TOF results were searched in MASCOT, which showed the presence of similar mass peptides in two different proteins. Among these two proteins, the first protein showed a 44% match with a score of 156 with biosynthetic arginine decarboxylase (UniProt ID: A0A3P4ATF2) from *T. thermophilus* (Figure 2). While the second protein showed only a 25% match with a score of 44 with DNA-directed RNA polymerase of *T. thermophilus*. This indicates that the purified protein is biosynthetic arginine decarboxylase from *T. thermophilus*.

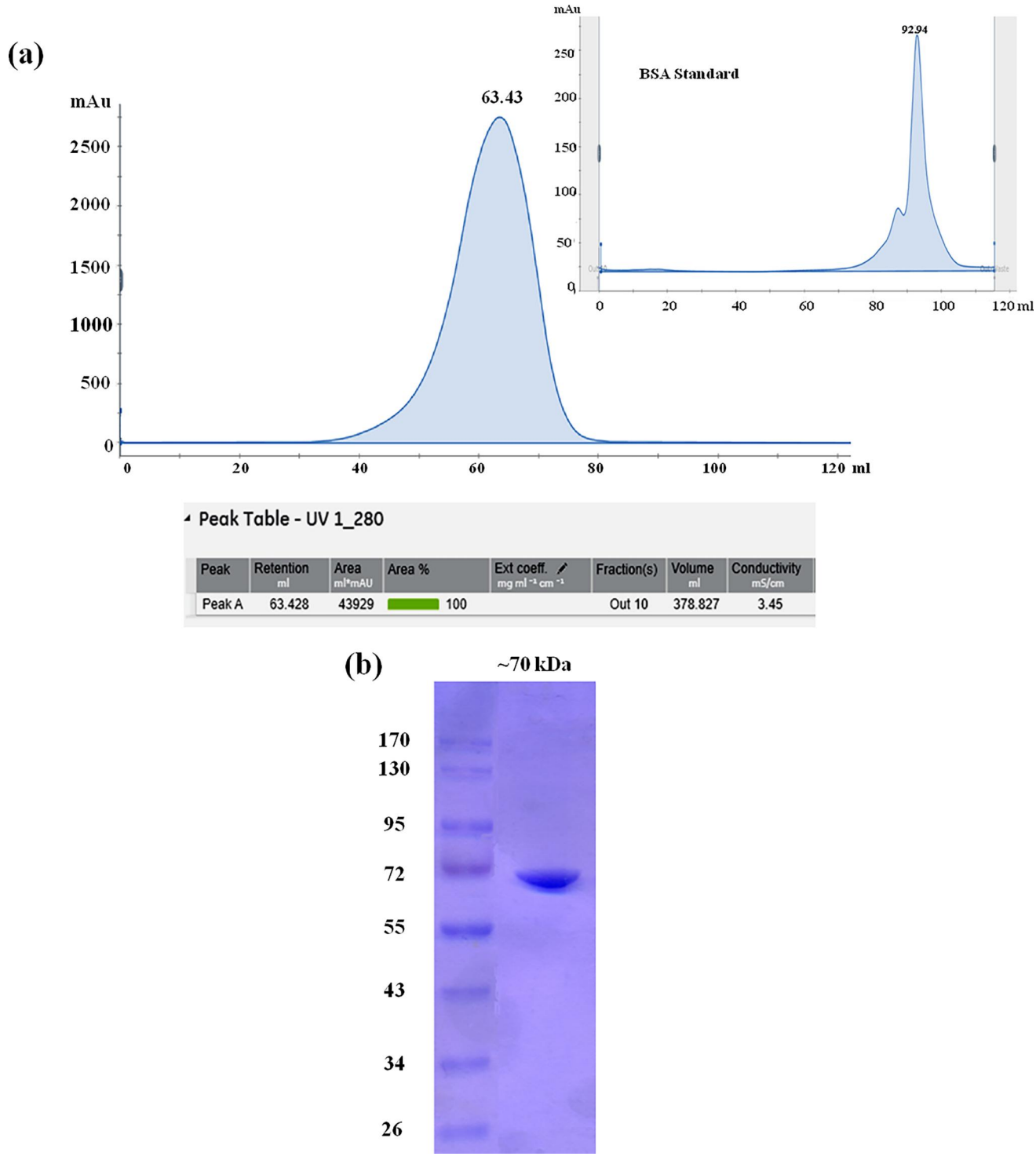

Figure 2. a) Analytical size exclusion chromatogram of purified TTHA1640 protein, b) SDS-PAGE profile for size exclusion chromatography purified protein. Lane: - Molecular weight standard, Lane 2: Purified protein by size exclusion chromatography (Peak1).

3.4. Determining the role of PLP in agmatine formation

The biosynthetic arginine decarboxylase was reported to catalyze the conversion of L-arginine substrate to arginine with the aid of PLP cofactor (Alam et al., 2018; Wu et al., 2015). To confirm the role of PLP and also to check whether the reaction happens without PLP, the activity assay was conducted with and without PLP. A slight increase in agmatine production was observed in the reaction with the addition of PLP. On the other hand, those without PLP also showed agmatine production (Figure 5a). In both cases, there is the formation of agmatine, but the addition of PLP enhances agmatine production.

3.5. Molecular docking with the cofactor PLP

The active site or binding site residues, crucial for the catalytic activity of the protein, are required for molecular interaction studies. Supporting this view, the conserved residue was identified based on the homologous sequences from

different organisms using the multiple sequence alignment (MSA) methods such as Clustal Omega (Sievers & Higgins, 2018). The MSA alignment unveiled the conservation of the lysine residue (Lys101) among Biosynthetic arginine decarboxylase of *T. thermophilus,* arginine decarboxylase of *E. coli* (PDB: 3NZQ_A), arginine decarboxylase from *Vibrio vulnificus* (PDB: 3N2O_A), and ornithine decarboxylase from *Homo sapiens* (PDB: 4ZGY), designating it as a critical site for conducting covalent docking with the PLP cofactor (Figure 3). The docking resulted in a high cdock affinity score of −9.696 kcal/mol (Table 1). The molecular interaction plot (Figure 6) indicated interactions of the phosphate group with Gly288 and Arg339 through hydrogen bonds and with Mg^{2+} *via* salt bridge interactions. Furthermore, the pyridoxal group forms one H-bond and a salt bridge interaction with Glu336, in addition to Glu124.

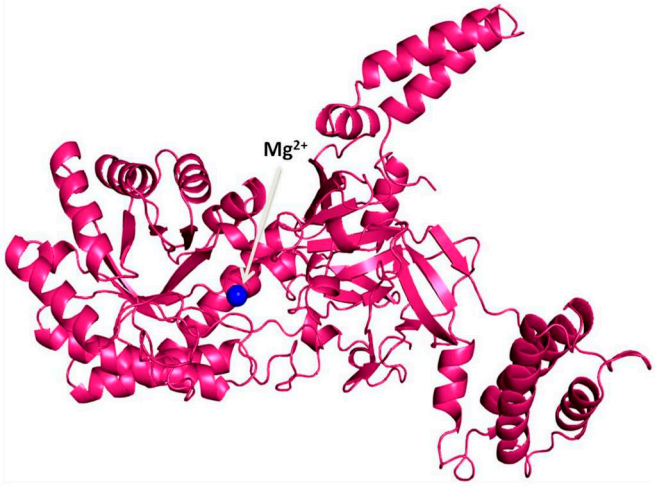

Figure 3. Modelled 3D structure of biosynthetic arginine decarboxylase (*Spe*A), with Mg^{2+} was fixed based on PDB ID: 4ZGY.

3.6. Time course experiment

The enzyme activity of biosynthetic arginine decarboxylase over time was determined by varying the incubation time. After each incubation, KOH was added to terminate enzyme activity, and readings were detected. This analysis inferred that, compared to the initial reading, there is an increase in agmatine production as the incubation time increases (Figure 5b). Increased agmatine production was observed at 1 hr incubation when compared to the initial reading. Thus, the remaining experiments were conducted with the same incubation time.

3.7. Effect of temperature on enzyme activity

T. thermophilus is known to survive in extreme temperatures in the range of 50 to 82°C (Friedrich et al., 2001). The effect of temperature on the activity of the biosynthetic arginine decarboxylase was examined by incubating it at different temperatures in the range of 20 to 90°C using a Peltier

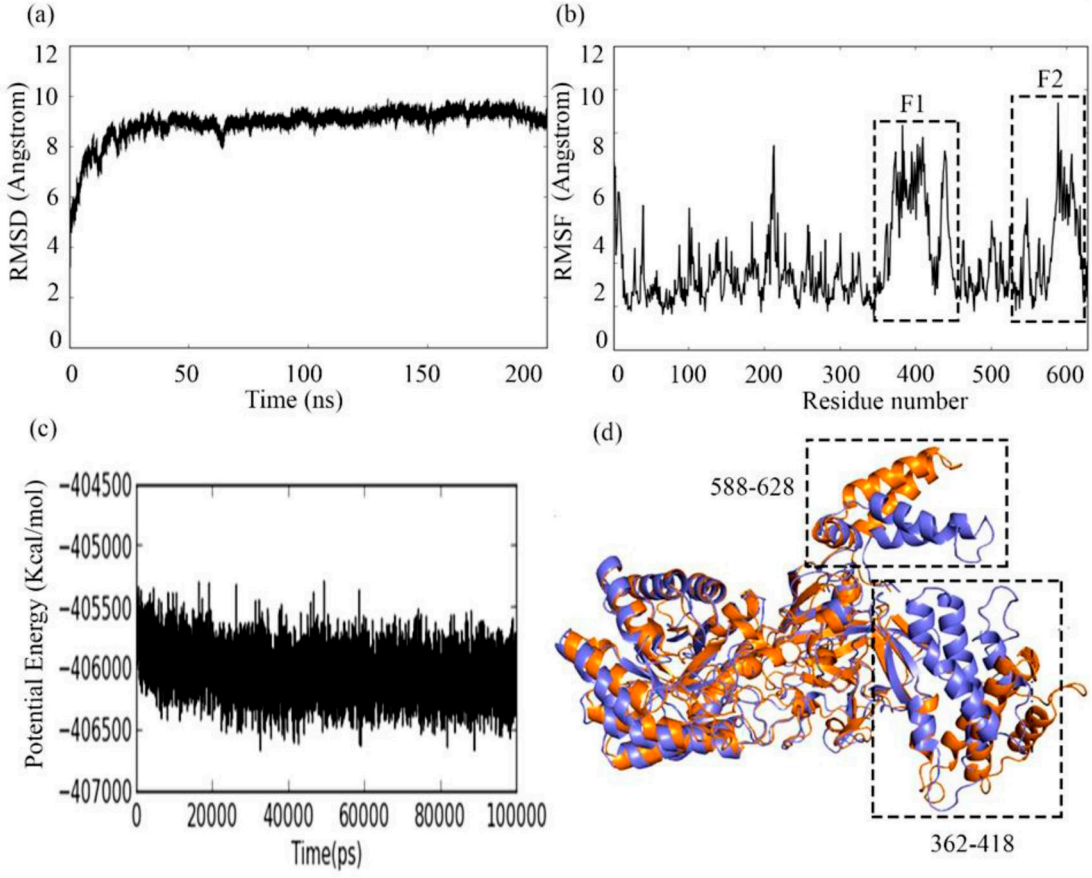

Figure 4. Molecular dynamics simulation analysis of *apo* biosynthetic arginine decarboxylase protein a) RMSD plot b) RMSF plot- the box represents the fluctuating residues c) Potential Energy of biosynthetic arginine decarboxylase, (d) comparative structural analysis of *apo* biosynthetic arginine decarboxylase initial (orange) and minimum potential structure (marine blue).

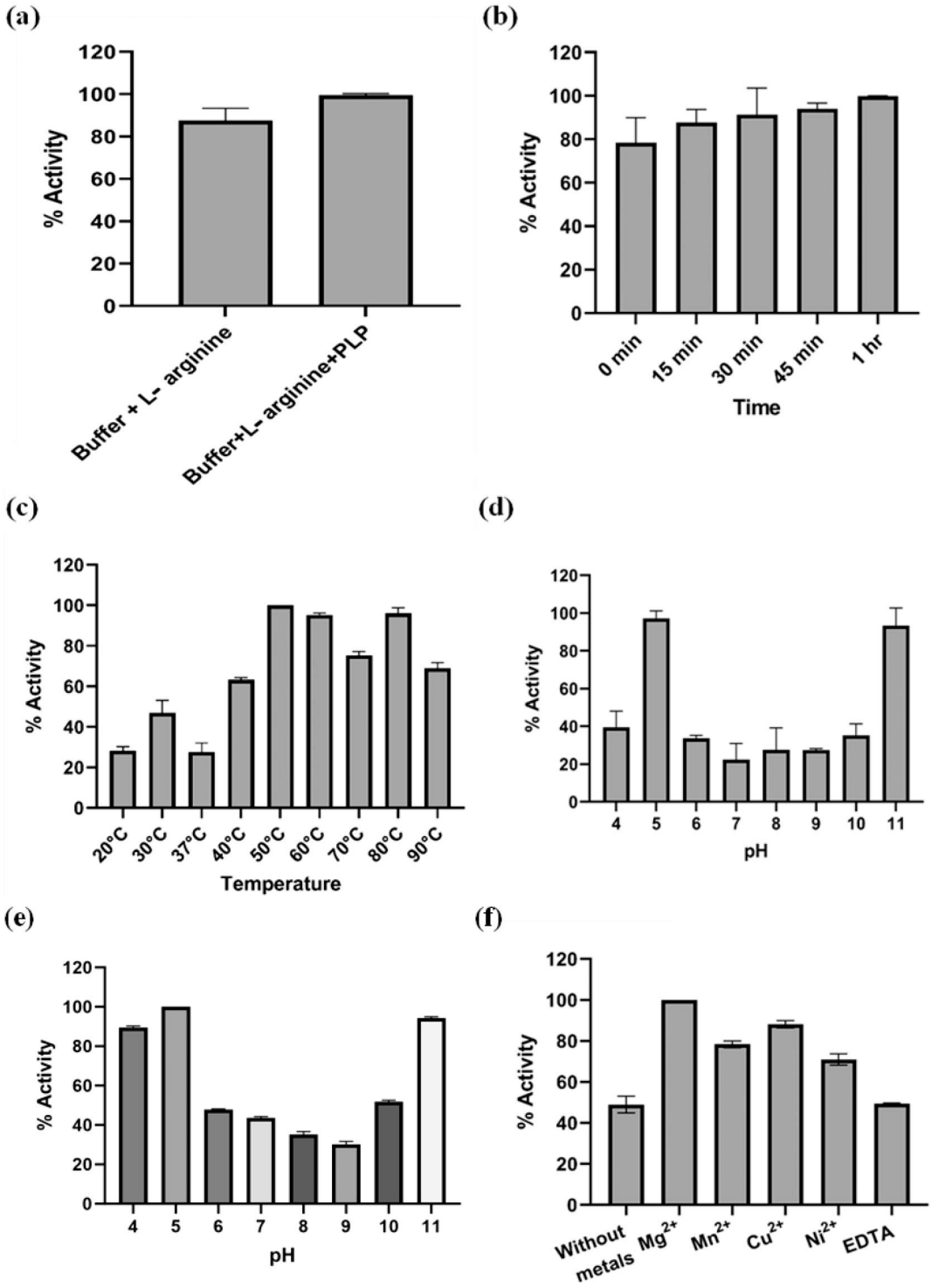

Figure 5. **(a)** Agmatine formation based on Cofactor, **(b)** The time-dependent activity assay of *T. thermophilus* biosynthetic Arginine decarboxylase was performed with enzyme and substrate at concentrations of 1 mM and 25 mM, respectively. The percentage of agmatine formed is plotted against time **(c)** Effect of temperature over the formation of agmatine, **(d)** Effect of pH on the formation of agmatine using Sodium phosphate buffer, **(e)** Effect of pH on the formation of agmatine using different buffer system **(f)** Ion-dependent behavior of the protein.

Table 1. Covalent docking analysis of Pyridoxal 5′-Phosphate (PLP) with biosynthetic arginine decarboxylase.

Complexes (Mg^{2+} + PLP)	glide gscore (kcal/mol)	cdock affinity (kcal/mol)	Docking score (kcal/mol)
1	−10.441	−9.696	−9.696
2	−10.38	−9.681	−9.681
3	−10.198	−9.337	−9.337

thermostat coupled with a spectropolarimeter. The concentration of enzyme and substrate was kept constant, and activity was measured. The higher activity of biosynthetic arginine decarboxylase was observed at 50°C, 60°C, and 80°C which implies that at a higher temperature, it has more activity (Figure 5c). Among these temperatures conditions, maximum activity was observed at 50°C compared to other

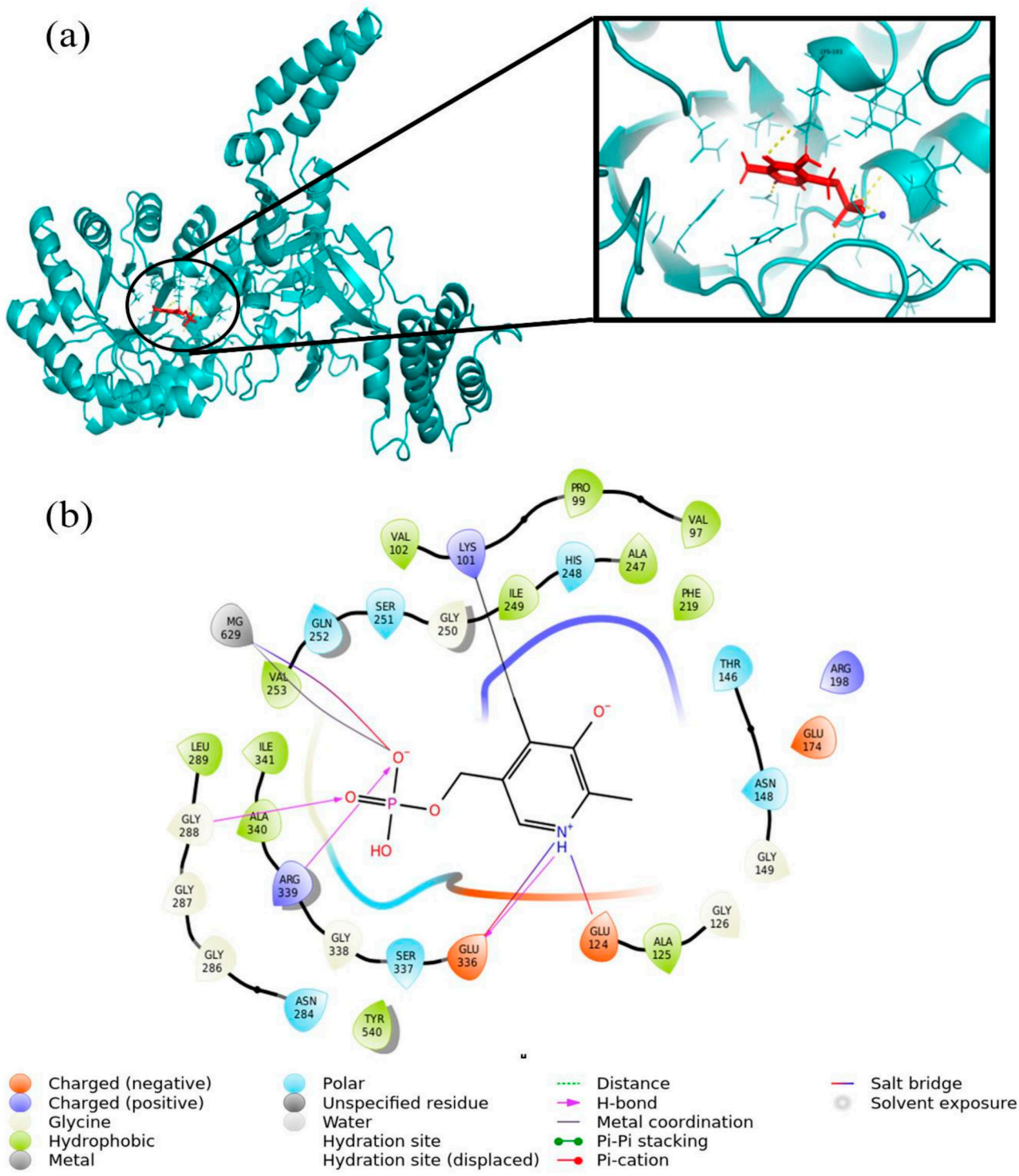

Figure 6. Molecular docking of Pyridoxal 5'-Phosphate (PLP) to the refined biosynthetic arginine decarboxylase.

temperatures. The present study is concurrent with the previous results, which reported that the arginine decarboxylase produced by *Helicobacter pylori* showed optimum activity at 50°C (Alam et al., 2018).

3.8. Temperature-dependent activity of biosynthetic arginine decarboxylase at varied pH ranges

To pinpoint and analyze potential sites in the structure of biosynthetic arginine decarboxylase, various MD simulations were conducted at higher temperatures, specifically 353.15K and 363.15K. This is because high temperatures can significantly impact the protein's structure and stability. Additionally, K et al., 2023, reported in their study TtArginase protein of *T. thermophilus* showed structural changes as the temperature increased (K et al., 2023). To infer these changes, the MD simulations were analyzed to evaluate the conformational stability and flexibility of the biosynthetic arginine decarboxylase under different physiological conditions.

3.8.1. MDS analysis of biosynthetic arginine decarboxylase at 300K with varied pH ranges

The structural stability metrics, RMSD and RMSF, were analyzed to assess the stability and conformational changes of the biosynthetic arginine decarboxylase at 300K under various pH conditions. Initially, the RMSD values were calculated from the residual backbone information to evaluate the difference in protein backbone over simulation time and to check the stability of the protein structure. As shown in Figure 7a, the RMSD ranges between 6.5 and 9.5 Å at neutral and alkaline pH, while an acidic pH resulted in a low RMSD value of 6 Å. Additionally, at neutral pH 7, the RMSD backbone pattern was observed to be well-equilibrated during the simulation, with an increased RMSD value of ∼9.5 Å. Typically, C terminal residues of the protein exhibit high mobility, and residues with high RMSF values undergo significant conformational changes. Figure 7b illustrates that the profiles of RMSF plots at different pH environments were similar, and two very flexible segments (F1 and F2), which included the residues Ile356-Pro468 and Thr574-Gly610, respectively, showed substantial mobility. The residual peaks reached more than 12 Å and 9 Å for the F1 and F2 peak regions, respectively.

3.8.2. MDS analysis of biosynthetic arginine decarboxylase at 323.15K with varied pH ranges

The RMSD plot at neutral pH 7 and alkaline pH 8 attained stability at the beginning itself, which persisted throughout the simulation, and not many changes were observed in these trajectories (Figure 7c). In the case of acidic pH 5, a low RMSD value of ∼5.2 Å has been observed with the stable equilibration pattern up to the simulation end. Further, it was observed that during the initial simulation phase for alkaline pH 11, the protein backbone RMSD increased up to a value of ∼12Å with respect to its initial structure and then stabilized around an average value of ∼8.2 Å for the remaining MD trajectories, indicating no change in the protein backbone. Further, the RMSF of Cα atoms was calculated for all the simulated trajectories of biosynthetic arginine decarboxylase at 323.15K with each pH studied, which is given in Figure 7d. Likewise, at 300K, the RMSF plots displayed highly flexible peaks with similar patterns for the majority of regions in the complexes (Figure 7d). The segments, comprising F1 (residues Glu346–Ser462) and F2 region (residues Arg570–Val607), are among the most fluctuating region of the biosynthetic arginine decarboxylase structure.

3.8.3. MDS analysis of biosynthetic arginine decarboxylase at 353.15 K with varied pH ranges

RMSD analysis of the backbone of biosynthetic arginine decarboxylase at 353.15K under various pH settings showed an RMSD value below ∼10 Å, except for pH 11, which indicates the stable behavior of simulated trajectories (Figure 7e). However, it is essential to note that from about ∼94 ns and up to the simulation end, all simulated trajectories displayed stable equilibration patterns. Subsequently, the local structural fluctuations displayed by the Cα atoms of the protein in response to different pH environments at 353.15K were investigated using residual RMSF analysis (Figure 7f). The segments, comprising F1 (residues Val352–Ala470), and F2 region (residues Arg570–Val607), are among the most fluctuating regions of the biosynthetic arginine decarboxylase structure.

3.8.4. MDS analysis of biosynthetic arginine decarboxylase at 363.15 K with varied pH ranges

From the resultant plots (Figure 7g), reliable trajectories were observed for the analyses as all systems exhibited well-equilibrated backbone patterns, except for pH 11, which had a flexible pattern around 10 to 125 ns. At an acidic pH of 5, the RMSD plot of protein backbone atoms reached stability at around 80 ns, and not many changes were observed during the simulation. In the case of backbone RMSD, the trajectories at neutral pH 7 were the most stable in the simulated time and noticed good overall stability with a low RMSD score of ∼9Å. At alkaline pH (pH 8 and 11), a gradual increase in RMSD values is observed in the simulation's initial phases in comparison to acidic and neutral pH. Following that, a stable pattern continued up to the simulation's end. Figure 7h depicts the per-residue flexibility dynamics of biosynthetic arginine decarboxylase protein at different pH environments. As shown in previous simulation settings, two regions (F1 and F2) demonstrated high flexibility with the RMSF value above ∼19 Å and ∼16 Å for F1 and F2 respectively. It can be seen from the residual RMSFs that pH 11 and pH 5 exhibited high flexible peaks in the F1 and F2 regions, respectively. However, compared to other systems, pH 7 and 8 showed relatively low RMSF values. For MDS analysis of biosynthetic arginine decarboxylase at 363.15K, no discernible pattern of changes was observed with an increase in pH.

3.9. Effect of pH on catalytic activity

The activity of biosynthetic arginine decarboxylase protein was examined by altering the pH of the buffer (30 mM $NaHPO_4$, 30 mM NaCl, 1.5 mM DTT, and 40 mM PLP) using fixed concentrations of substrate and protein. As shown in Figure 5d, we observed optimum activity at pH 5. Also, pH 11 showed good activity next to pH 5. The optimum activity at pH 5 is concurrent with the *E. coli* arginine decarboxylase which showed optimal activity at pH 5.2 (Blethen et al., 1968). Also, we hypothesize that the activity of the enzyme at pH 11 with the L-arginine substrate could be due to its protonation at basic pH. Earlier studies have reported that protonation of Histidine amino acid can increase the substrate binding in the conformational flexibility of transcription factors protein (Narayan & Naganathan, 2018). At pH 11, His248: Hie, Arg339: Positively Charged, Glu336: Negatively Charged, amino acids that interacted with the substrate were protonated. Since in the present study, the substrate itself is an amino acid and therefore the protonation would have increased the interaction of L-arginine substrate, at pH 11. The protein showed its optimum enzyme activity at both conditions acidic and basic. According to Morris & Pardee,

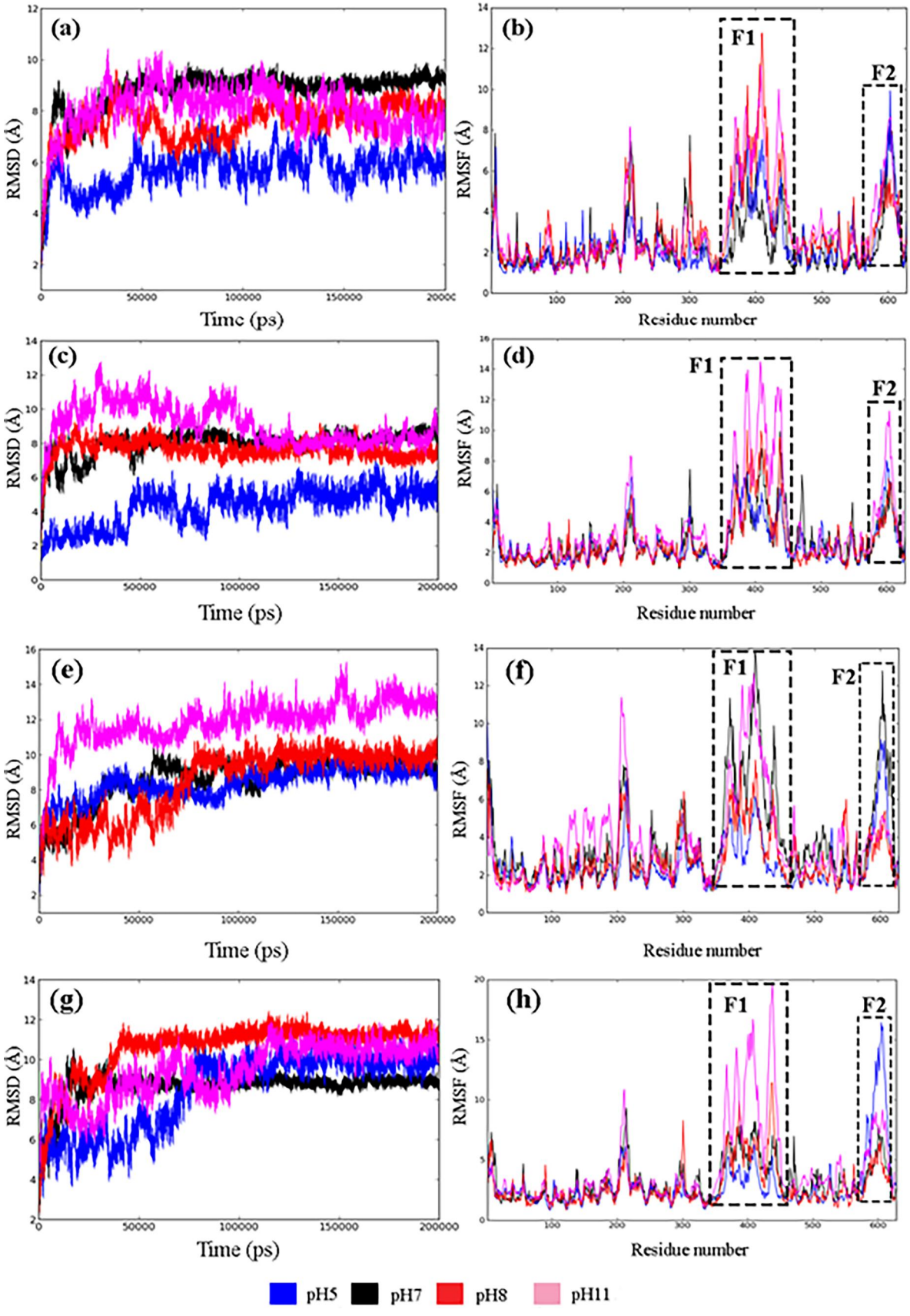

Figure 7. Comparative RMSD analysis of biosynthetic arginine decarboxylase under different pH conditions at (a) 300 K (c) 323.15 K (e) 353.15 K (g) 363.15K, and Comparative RMSF analysis of biosynthetic arginine decarboxylase under different pH conditions at (b) 300 K (d) 323.15 K (f) 353.15K (h) 363.15K.

1965 the arginine decarboxylase in *E. coli,* showed optimum activity at pH 8. In contrast to their report Blethen et al., 1968 reported that inducible *E. coli* arginine decarboxylase shows optimal activity at pH 5.2. Also in another report by Alam et al., 2018 *H. pylori* arginine decarboxylase shows its optimum activity at pH 8.5, while *H. pylori* arginase, which uses the same substrate L-arginine, showed optimal activity at pH 6.1. These reports evidence to the fact that the arginine decarboxylase is capable of showing its optimum activity at both acidic and basic pH.

The same assay was repeated by varying the buffer system (30 mM buffer based upon pH, 30 mM NaCl, 1.5 mM DTT, and 40 mM PLP) in order to cross-check the activity of the protein using different buffers. The Citrate buffer, Tris-HCl, Glycin-sodium hydroxide (NaOH), and Sodium bicarbonate ($NaHCO_3$)-Sodium hydroxide (NaOH) buffers were used to check the activity, these buffers were selected based on their physiological pH range and buffering capacity. The different buffer system assay results showed its optimum 100% activity at pH 5 (Figure 5e) same as it was observed in the case of constant Sodium Phosphate ($NaHPO_4$) buffer (Figure 5d). Also, next to that pH 11 showed 94.25% activity, this result also correlates with the constant buffer system result. An unlikely increase in activity of the protein was observed in citrate buffer at pH 4 (89.5%), which was not observed in the case of Sodium Phosphate ($NaHPO_4$), this might be due to the changes in the buffer system. Altogether, more activity was observed at pH 5 and pH 11 hence, from both assays this was concluded to be the optimum suitable pH for agmatine production.

3.10. Effect of pH and temperature on biosynthetic arginine decarboxylase stability and activity

The MD simulation was explicitly carried out to comprehend the structural level changes and structural stability of biosynthetic arginine decarboxylase under different temperature settings (300K, 323.15K, 353.15K, and 363.15K). Structural stability and flexibility metrics, RMSD and RMSF, were used to explore the changes in the structural stability of biosynthetic arginine decarboxylase at different physiological conditions. The MD simulation results correlate with the obtained enzymatic activity of biosynthetic arginine decarboxylase *in vitro* and provide a deep insight into the conformational dynamics of the protein at the same temperature and pH environments.

3.10.1. MDS analysis of biosynthetic arginine decarboxylase at acidic pH 5 under varied temperatures

Assessment of stability through RMSD and RMSF: Two structural stability metrics, RMSD and RMSF, were used to confirm the structural stability of biosynthetic arginine decarboxylase complexed with its PLP cofactor. RMSD stands for the distance of the atoms in the protein backbone from its initial configuration. The backbone RMSD profile clearly showed that the 323.15 K had the least variation (∼4.5 Å), while the 363.15 K had the highest deviation of ∼10.5 Å (Figure 8a). The remaining temperature simulation trajectories showed slight variation in the simulation period. The RMSD profile has inferred that the structural stability of biosynthetic arginine decarboxylase significantly declined at high-temperature conditions (353.15 and 363.15 K) besides moderate strength stability, moderate strength at room temperature (300K), and strong stability at 323.15 K. The RMSF parameter describes the flexibility of the protein and aids in understanding dynamic motion during MD. Lower RMSF values represent the protein's restricted region. In contrast, the more flexible portions of the protein are indicated by a larger RMSF value. Each residue's RMSF value in biosynthetic arginine decarboxylase was computed at pH 5 with various temperature settings (Figure 8b). However, RMSF values of the residues were higher in two regions, denoted in the plot as F1 (Ala340 to Pro488) and F2 (Val580 to Gly610), respectively. The F1 region showed reduced RMSF values in the range of ∼2Å to 7.5 Å, while the C-terminal residues occupying the F2 region demonstrated an increased RMSF value up to 16 Å. The residues at high temperatures, 323.15 and 363.15 K represented maximal fluctuating residues in the F2 region. Therefore, it is evident that high temperatures (353.15 and 363.15 K) can cause substantial damage to the protein conformation by exhibiting reduced structural stability and increased flexibility. The RMSD and RMSF results also established that biosynthetic arginine decarboxylase was highly stable and least flexible at acidic pH 5 and had optimum activity at 323.15K.

3.10.2. MDS analysis of biosynthetic arginine decarboxylase at neutral pH 7 under varied temperatures

The structural dynamics of biosynthetic arginine decarboxylase at neutral pH 7 under different temperatures were obtained by analyzing the backbone RMSD (Figure 8c). At neutral pH, except for 323.15 K, biosynthetic arginine decarboxylase exhibited a substantially high RMSD value, denoting structural instability. However, in high-temperature settings (353.15 and 363.15 K), the RMSD values of protein systems fall within a similar range (deviation range: ∼8 to 10 Å), which is consistent with the outcomes of the acidic pH. Additionally, the room temperature (300 K) displayed a high RMSD value of ∼9.8 Å, which contradicts acidic pH. The individual residual dynamics examined by RMSF (Figure 8d), were found compatible with RMSD, evidencing that biosynthetic arginine decarboxylase could acquire significant structural changes in response to temperature changes with the presence of two highly flexible peaks (F1:Ala340 - Pro478 and F2:Val580 - Gly610) in the plot. Moreover, compared to acidic pH, a high flexible peak was observed in the regions of F1 at the neutral pH condition. Further, the residual RMSF analysis showed significant structural fluctuations on increasing the temperature from 300 K. On increasing the system's temperature, the fluctuation was formed more for 353.15 and 363.15 K, while less fluctuation was observed at 300 K. The results obtained from RMSD and RMSF analysis for the biosynthetic arginine decarboxylase at neutral pH under various temperatures indicate that in the high temperatures (353.15 and 363.15 K), the structural flexibility was higher than at 300 K and 323.15 K.

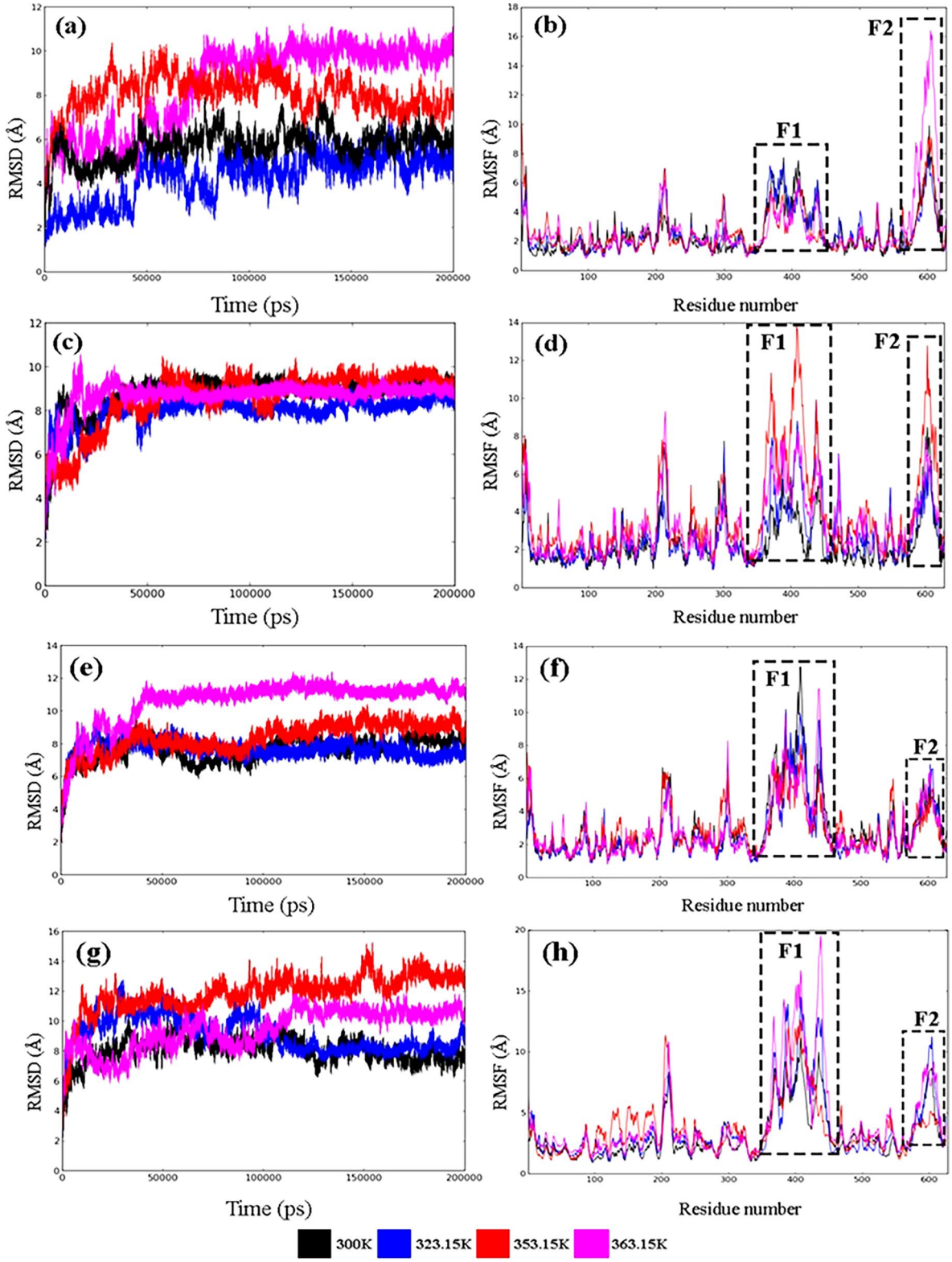

Figure 8. Comparative RMSD analysis of biosynthetic arginine decarboxylase under different temperature conditions at (a) pH 5 (c) pH 7 (e) pH 8 (g) pH 11; Comparative RMSF analysis of biosynthetic arginine decarboxylase under different temperature conditions at (b) pH 5 (d) pH 7 (f) pH 8 (h) pH 11.

3.10.3. MDS analysis of biosynthetic arginine decarboxylase at alkaline pH 8 under varied temperatures

Through backbone RMSD analysis at various temperatures, the structural stability of biosynthetic arginine decarboxylase at alkaline pH 8 was examined. The RMSD plot (Figure 8e) shows that the RMSD values are substantially greater at high temperatures (353.15K and 363.15 K) compared to room temperature (300 K) and with the RMSD obtained at 323.15 K. Similar to acidic and neutral pH, higher temperatures (353.15 and 363.15 K) at alkaline pH exhibited structural instability during the simulation. The RMSD analysis showed the lowest RMSD at 323.15 K indicating maximum stability. Further, a

distinct pattern of reduced structural stability of biosynthetic arginine decarboxylase protein with increasing temperature (300K→363.15K) has been noted in this condition. The residual dynamics were explored using the RMSF analysis (Figure 8f) highlighted a single high flexible peak (F1) in the plot, corresponding to residues from Pro367 to Pro488. In addition, the highly flexible peak (F2), observed in a neutral pH condition, was reduced in this alkaline condition. Similar to acidic and neutral pH conditions, decreased structural stability was observed at higher temperatures (353.15K and 363.15K) in an alkaline condition. Moreover, reduced flexible peaks in the F2 region and significant structural changes were observed following the shift in pH (from neutral to alkaline condition).

3.10.5. MDS analysis of biosynthetic arginine decarboxylase at basic pH 11 under varied temperatures

The RMSD profile (Figure 8g) was calculated at pH 11 under varied temperatures and was found to display a similar equilibration profile. It was clear that structural deviation is significantly increased for the higher temperatures (353.15 and 363.15 K) than the 300 K and 323.15K throughout the simulation period, which may be associated with the increased molecular mobility under this condition. Although it is widely known that temperature affects atomic fluctuation, the influence of temperature on protein varies. The RMSD results were further supported by a significant increase in RMSF value (∼up to 20 Å) in the protein Cα atoms of 353.15 and 363.15 K (Figure 8h). Further, a decreased residual mobility was observed in the conserved F2 region (residues from Val580 - Gly 610), which indicates that the change in pH from neutral to alkaline condition suppresses the high flexible peaks in this region.

Overall, the findings of RMSD analysis under alkaline conditions evidenced that an increase in temperature leads to structural instability when compared to room temperature (300 K and 323.15 K). Moreover, the RMSF analysis confirmed that biosynthetic arginine decarboxylase under alkaline conditions showed structural conformational changes induced by the shifting of pH from neutral to alkaline.

3.11. Effect of ions on enzyme activity

As per the reports of earlier studies, the biosynthetic arginine decarboxylases require PLP and Mg^{2+} ions as cofactors for their activity (Alam et al., 2018). Hence, the effects of external metal on the activity of biosynthetic arginine decarboxylase were investigated by using various metal ions (Mg^{2+}, Cu^{2+}, $Mn^{2+,}$ and Ni^{2+}) in the concentration of 5 mM. In the absence of metal, it showed minimal catalytic activity, also even upon the addition of EDTA it showed the same. However, in the presence of Mg^{2+}, the enzyme produced maximum agmatine production which is in accordance with the previous reports supporting that metal binding is required to speed up the reaction. To determine whether other divalent metals can also aid this reaction, Mn^{2+}, Cu^{2+}, and Ni^{2+} were added to the experiment. The other metals also enhanced the activity in the following order: $Mg^{2+} > Cu^{2+} > Mn^{2+} > Ni^{2+}$ (Figure 5e). The metals we used in the ion-dependent assay are divalent metals that have a 2^{+} oxidation state which means they can lose two electrons. With this property, these metals might participate in electron transfer reactions which facilitate electron movement and play a role in substrate binding, activation, and stabilization. They would have formed coordination bonds with amino acid side chains or backbone atoms, enhancing the protein's catalytic efficiency. This might be the reason for its positive activity in the presence of other ions. In *Helicobacter pylori* arginine decarboxylase also they have observed 100% activity in the presence of Mg^{2+} and 80% in Mn^{2+} which coordinates with our result indicating that not only Mg^{2+} but also other divalent metals can act as a cofactor for activity of the protein (Alam et al., 2018). Though other metals can enhance the reaction, Mg^{2+} is more efficient than others in aiding the reaction with optimal enzymatic activity.

3.12. Molecular docking of biosynthetic arginine decarboxylase with its substrate at different physiological conditions

In order to determine the catalytic activity of biosynthetic arginine decarboxylase with its L-arginine (substrate), the GLIDE docking was performed in Schrödinger suite version 2022. The low potential energy conformation of the biosynthetic arginine decarboxylase protein - PLP cofactor complexes at various pH and temperature settings were used for molecular docking analysis to attain structural insights into these complexes. The XP docking score (kcal/mol) and MMGBSA binding energy score (kcal/mol) of each biomolecular complex are given in Table 2. It is widely accepted that molecular interactions are necessary to maintain the protein structure stable and compact. The molecular interactions formed by the substrate molecule with PLP cofactor and substrate binding pocket residues are listed in Table 3. **pH 5:** The molecular interaction of biosynthetic arginine decarboxylase with the L-arginine substrate exhibited the XP docking scores of −3.64, −5.29, −4.53, and −1.43 kcal/mol for 300K, 323.15K, 353.15K, and 363.15K, respectively. The interaction analysis of biosynthetic arginine decarboxylase with

Table 2. Molecular Docking Analysis of biosynthetic arginine decarboxylase with L-arginine (substrate).

Complexes	XP score (kcal/mol)	MMGBSA (kcal/mol)
pH 5 300K	−3.64	−12.67
pH 5 323.15 K	−5.29	−10.27
pH 5 353.15 K	−4.53	−19.85
pH 5 363.15 K	−1.43	−17.48
pH 7 300K	−5.36	−36.90
pH 7 323.15K	−2.84	−43.82
pH 7 353.15K	−4.80	−43.82
pH 7 363.15K	−4.72	−29.26
pH 8 300K	−4.63	−27.42
pH 8 323.15K	−4.80	−43.41
pH 8 353.15K	−4.34	−41.18
pH 8 363.15K	−5.23	−30.81
pH 11 300 K	−5.935	−16.20
pH 11 323.15 K	−4.051	−25.61
pH 11 353.15 K	−2.798	−15.63
pH 11 363.15 K	−3.958	−26.82

Table 3. Molecular interaction of biosynthetic arginine decarboxylase with substrate and cofactor.

Protein Complex	Hydrogen bond	Salt bridge	Pi-cation
pH 5 300K	Gly 250, Ile 247, and PLP	PLP	PLP
pH 5 323.15 K	Tyr 293, Glu 336, Ser 337, and PLP	Mg^{2+}, PLP	
pH 5 353.15 K	Gly 288, Hie 248, and PLP	PLP	
pH 5 363.15 K	Ser 251, Lys 204, Gln 252, and Thr 254	Lys 204	
pH 7 300K	Glu 215, Asn 216, Glu 336, and PLP	Glu 215, PLP	
pH 7 323.15K	Ser 303, Tyr 306, and Gly 250	PLP	
pH 7 353.15K	Tyr 306, Asn 305, Glu 475, Asp 292, and Lys 297	Lys 297, Asp 292, Arg 339	Tyr 306
pH 7 363.15K	Gly 287, Leu 289, and PLP	Glu 336, Asp 469, PLP	
pH 8 300K	Gly 287, and PLP	PLP	
pH 8 323.15K	Tyr 301, and PLP	Lys 101, PLP	
pH 8 353.15K	Gly 214, Arg 339, Asp 292, Ala 290, and PLP	Glu 215, Asp 292, Arg 339, PLP	
pH 8 363.15K	Glu 215, Val 291, Tyr 293, and PLP	Glu 215, Arg 339, PLP	Tyr 293
pH 11 300 K	Gly 287, Ser 251, and PLP	PLP	
pH 11 323.15 K	Glu 336, Hie 248, Gly 287, and PLP	PLP	
pH 11 353.15 K	Gly 287, Glu 336, Leu 289, and Arg 339		
pH 11 363.15 K	Tyr 301, Gln 252, and Thr 254		

L-arginine substrate revealed that at 323.15K, there were a high number of intermolecular interactions, including four hydrogen bonds, three salt bridges, and one metal coordination, which are listed in Table 3 and plotted in Figures 4. In all of the complexes, except for 363.15K, molecular interactions were consistently formed between the L-arginine substrate and PLP cofactor. Moreover, the docked complex exhibited a lower docking score of −1.43 kcal/mol, at 363.15K, which can be correlated with its high RMSD deviation and less structural stability. **pH 7:** The molecular docking scores at different temperature conditions ranged between −2.84 and −5.36 kcal/mol (Table 3). The complex at 300K showed the highest docking score of −5.36 kcal/mol and the 323.15K complex exhibited the lowest docking score of −2.84 kcal/mol, evidencing their intermolecular interactions (Fig. S5). Moreover, the complex at 353.15K did not show any intermolecular interaction between the PLP cofactor and L-arginine substrate, even though it exhibits a comparable docking score of −4.80 kcal/mol. In the 363.15K complex, three HBs and one SB interaction were found to be involved in binding the PLP cofactor with the substrate molecule. Additionally, three Hydrogen bond (HBs) with Gly287, Leu289, and Asp 469 and two salt bridge (SB) interactions with Glu336 and Asp469 were found to stabilize the docked complexes by exhibiting a docking score of −4.72 kcal/mol. **pH8:** The binding modes of the substrate molecule at different temperature conditions (300K, 323.15K, 353.15K, and 363.15 K) are represented in Figure 6. In this alkaline pH environment, persistent interactions were observed between the PLP cofactor and L-arginine substrate under all temperature conditions, in which both HBs and SBs were actively engaged in the stabilization of the complexes. The molecular docking results showed that the substrate molecule can bind effectively at 363.15K through HB and SB interactions between PLP cofactor and biosynthetic arginine decarboxylase. The molecular interaction analysis demonstrated that residue Glu215 at 363.15K complex participated in HB and SB interactions. Meanwhile, Tyr293 was actively engaged in π-cation interaction with the substrate molecule. When docked with biosynthetic arginine decarboxylase at 353.15K, the substrate molecule showed a relatively low docking score of −4.34 kcal/mol. **pH 11:** The XP docking score for the interaction between biosynthetic arginine decarboxylase and L-arginine substrate was found to be −5.93, −4.05, −2.79, and −3.95 kcal/mol for 300K, 323.15K, 353.15K, and 363.15 K, respectively. The complex at 300K showed a relatively high binding affinity with a docking score of −5.93 kcal/mol due to the presence of an increased number of five HBs and two SBs contributing to the complex stability (Figure 7). The significant difference in the intermolecular interactions in this alkaline pH condition compared to other pH environments is that no interaction formed between PLP and L-arginine at two 353.15K and 363.15K. Compared to other complexes, the 363.15K had fewer HBs and salt bridges, and the MD simulation showed that the complex also lost structural stability and acquired high flexibility.

The molecular docking simulation results evidenced the binding mechanism of substrate molecules under various physiological conditions, especially the role of molecular interactions in upholding the stability and compactness of the protein structure.

3.13. MDS analysis on biosynthetic arginine decarboxylase complexed with its L-arginine substrate

The molecular binding of a ligand/substrate at the binding pocket of a protein might cause several conformational changes in the structure of the protein. Therefore, to analyze how the binding of L-arginine substrate can alter conformational flexibility, and to study the stability of biosynthetic arginine decarboxylase L-arginine substrate complexes, a long-range MD simulation was performed for 200 ns aimed at the two best-docked complexes observed in both *in vitro* and *in silico* analysis.

Complex dynamics pH 5 323K: In MD simulations, RMSD measurements are frequently utilized as indicators of structural variation over time in 3D space. While high RMSD values signify structural instability and low RMSDs reflect structural stability. The structural stability of L-arginine substrate-bound complexes was investigated using stability indicator tools such as RMSD and RMSF. Initially, the RMSD values for the alpha carbon (Cα) atoms of biosynthetic arginine decarboxylase and the substrate were computed to measure the average change in displacement with respect to the initial frame. In Figure 9a, the Cα atoms dynamics of

biosynthetic arginine decarboxylase protein in complex with its substrate molecule started fluctuating in the initial phase of simulation (up to ~40 ns), gained stability afterward, and remained stable throughout the simulation. Moreover, similar stable trajectories were also attained in their *apo* form under this condition. Notably, stable conformational dynamics were observed for the substrate till ~50 ns; afterward, a drastic high RMSD was observed after ~80 ns and did not equilibrate till the end of simulation run. However, the initial stable trajectory of the substrate molecule in the complex indicates that the substrate is spatially well-occupied and stabilized with the molecular contacts at the binding pocket of biosynthetic arginine decarboxylase. The results of RMSD were supported by residual RMSF are illustrated in Figure 9b. Likewise, in the *apo* form, a similar fluctuation pattern was observed for the substrate-bound complex, which demonstrated two highly flexible peaks, F1 and F2, in the plot. The residues around His372—Tyr426 are located in the F1 region, whereas the residues occupy the F2 region from Val580 to Ser605. Further, the RMSF values for Cα atoms at the substrate binding site are found to be in the range of ~0.6 Å to 6.4 Å with the absence of high peaks at N and C-terminal residues, which reflect a reduced degree of flexibility in the substrate binding region. This finding demonstrates that the ligand movement is stable throughout the simulation.

Complex dynamics pH 11 at 300K: The Cα-RMSD of the biosynthetic arginine decarboxylase complex demonstrated that the enzyme attained stability very quickly. The complex trajectories reveal an initial rise in RMSD of ~4.8 Å, which settled gradually, and a stable equilibrium can be seen up to 155 ns; following that, a sharp increase in RMSD was noted up to ~6.1 Å; afterward, the system maintained constant equilibrium pattern until the end of the simulation (Figure 10a). In this complex dynamics, the substrate in the binding pocket remains stably associated with the biosynthetic arginine decarboxylase structure during the simulation's initial phase (up to 170 ns), after which there was a short period of time (~160 to 175 ns) during which there was a sudden RMSD deviation of the substrate, however, it has maintained steadily in the last ~20 ns. In addition, the RMSF plot (Figure 10b) further demonstrated the structural flexibility of the biosynthetic arginine decarboxylase protein. The residual dynamics based on Cα atoms showed a similar fluctuation pattern as seen in the *apo* protein, which showed a single high flexible peak in the plot with the absence of a conserved peak at the C-terminal region. While in the complex

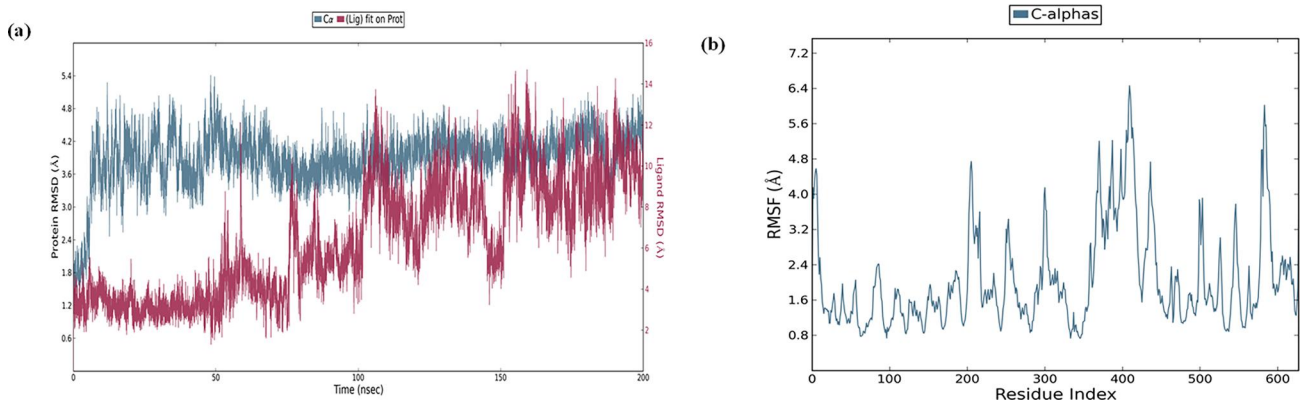

Figure 9. MD analysis of pH 5 at 323.15K (a) RMSD plot (b) RMSF plot.

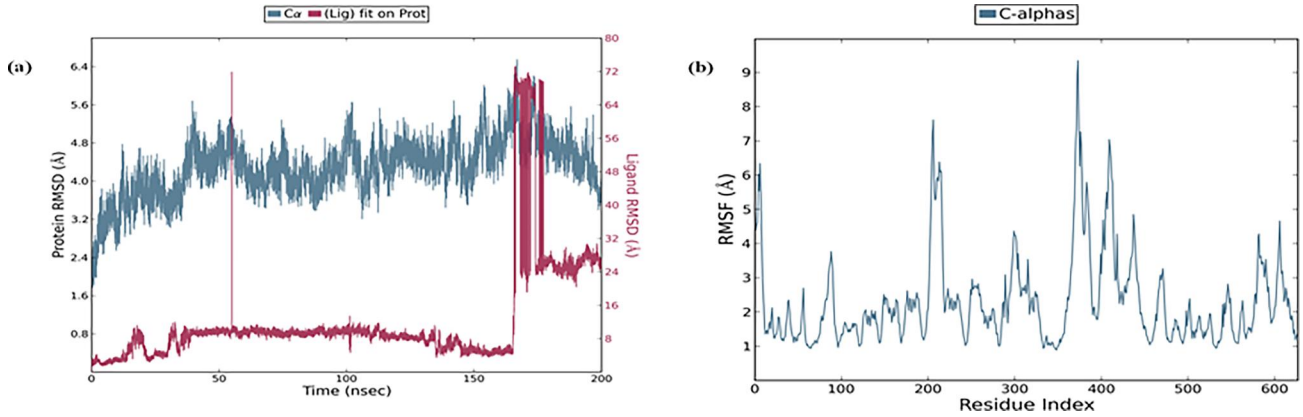

Figure 10. MD analysis of pH 11 at 300K (a) RMSD plot (b) RMSF plot.

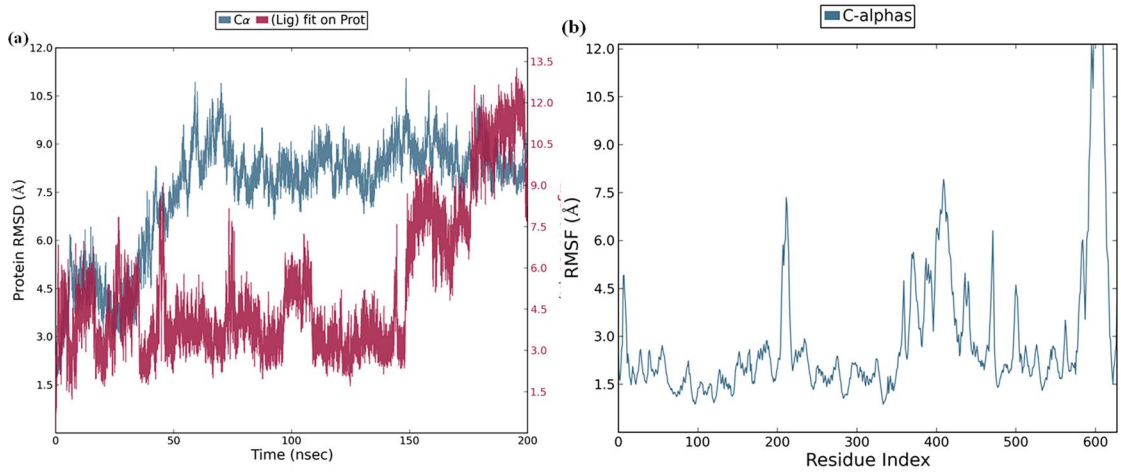

Figure 11. MD analysis of pH 11 at 323K (a) RMSD plot (b) RMSF plot.

dynamics of pH 5 at 323K, two highly flexible peaks were observed, which suggests structural changes in this region of biosynthetic arginine decarboxylase in response to shifting in pH (acidic to basic).

Complex dynamics pH 11 at 323K: The RMSD plot corresponding to the Cα atoms of biosynthetic arginine decarboxylase L-arginine substrate complex revealed that the substrate molecule was not firmly held in the binding pocket from the initially docked poses. The trajectories of Cα atoms showed a gradual increase in RMSD value during ~30-65 ns; following that, steady RMSD trajectories were maintained throughout the simulation. Additionally, utilizing the ligand (substrate) RMSD, the dynamics of the substrate were evaluated after it had bound with the substrate binding pocket (Figure 11a). Overall, the substrate exhibited varied behavior during the simulation. The substrate was observed in a lower dynamic range (below 5Å) across the simulation time, except towards the end, where the substrate achieved a slightly higher deviation (~11 Å) than the Cα atoms of biosynthetic arginine decarboxylase structure. Further, the flexibility of the biosynthetic arginine decarboxylase residues following contact with its L-arginine substrate is investigated using residual RMSF. The RMSF values for Cα atoms at the substrate binding site are found to be in the range of 1 Å to 8 Å, except in the C-terminal residues (above 12Å), which reflect a reduced degree of flexibility in the binding region (Figure 11b).

4. Conclusions

Biosynthetic arginine decarboxylase from *T. thermophilus* was successfully cloned, expressed, and purified, with a molecular weight of 70.24 kDa. This protein is involved in the biosynthesis of polyamines, including spermidine, which exhibits a wide range of biological activities, and its potential biotechnological applications are of great interest. Using biological assays, we investigated the enzyme's activity under different physiological conditions (varied pH, temperature, and ions). Additionally, we analyzed the dynamic behavior of the protein under varying physiological conditions using *in silico* studies. MALDI-TOF analysis confirmed that the purified protein is biosynthetic arginine decarboxylase involved in Spermidine production. Results from the time-dependent assay revealed that the enzyme activity increased with incubation time. Furthermore, the enzyme activity assay showed optimal activity at acidic (pH 5) and basic (pH 11) pH conditions and a temperature of 50 °C. Due to the demands of industrial production, natural enzymes are not sufficient. Therefore, engineered enzymes are the preferred option. Hence the study finding in terms of optimum pH, temperature, and cofactor could be of great help in the production of this enzyme on a large.

Acknowledgment

JJ acknowledges DST INDO-TAIWAN (GITA/DST/TWN/P-86/2019), Department of Biotechnology- Bioinformatics Centre (BIC)-No.BT/PR40154/BTIS/137/34/2021, DBT-NNP N0.BT/PR40156/BTIS/137/54/2023, TANSCHE (RGP/2019-20/ALU/HECP-0049dated:27/04/2021), DST- Fund for Improvement of S&T Infrastructure (FIST) (SR/FST/LSI-667/2016) (C), and DST-Promotion of University Research and Scientific Excellence (PURSE phase II) (No. SR/PURSE Phase 2/38(G), 2017), MHRD-RUSA 2.0, New Delhi (F.24e51/2014-U, Policy (TNMulti-Gen). VM thank ICMR for providing financial assistance through ICMR/SRF Fellowship (BMI/11(103)/2022).

Disclosure statement

The authors declare no conflict of interest.

Funding

JJ acknowledges DST INDO-TAIWAN (GITA/DST/TWN/P-86/2019), Department of Biotechnology- Bioinformatics Centre (BIC)-No.BT/PR40154/BTIS/137/34/2021, DBT-NNP N0.BT/PR40156/BTIS/137/54/2023, TANSCHE (RGP/2019-20/ALU/HECP-0049 dated:27/04/2021), DST- Fund for Improvement of S&T Infrastructure (FIST) (SR/FST/LSI-667/2016) (C), and DST-Promotion of University Research and Scientific Excellence (PURSE phase II) (No. SR/PURSE Phase 2/38(G), 2017), MHRD-RUSA 2.0, New Delhi (F.24e51/2014-U, Policy (TNMulti-Gen). VM thank ICMR for providing financial assistance through ICMR/SRF Fellowship (BMI/11(103)/2022).

Authors contribution

VM, KA, HN have designed the research. VM and KA conducted the *in vitro* experiments and VM, HN and KA have done *in silico* analysis. KA and MJ have wrote the paper. All the authors have read and approved the manuscript.

Data availability statement

Despite the reason of sensitivity, the data supporting this study are not openly, but are available upon reasonable request to the corresponding author.

References

Alam, M., Srivastava, A., Dutta, A., & Sau, A. K. (2018). Biochemical and biophysical studies of Helicobacter pylori arginine decarboxylase, an enzyme important for acid adaptation in host. *IUBMB Life*, *70*(7), 658–669. https://doi.org/10.1002/iub.1754

Altschul, S. F., Gish, W., Miller, W., Myers, E. W., & Lipman, D. J. (1990). Basic local alignment search tool. *Journal of Molecular Biology*, *215*(3), 403–410. https://doi.org/10.1016/S0022-2836(05)80360-2

Arora, N. K., Agnihotri, S., & Mishra, J. (2022). Extremozymes and Their Industrial Applications. Elsevier Science & Technology. https://ebookcentral.proquest.com/lib/kxp/detail.action?docID=7018202

Bae, D. -H., Lane, D. J. R., Jansson, P. J., & Des Richardson, R. (2018). The old and new biochemistry of polyamines. *Biochimica et Biophysica Acta. General Subjects*, *1862*(9), 2053–2068. https://doi.org/10.1016/j.bbagen.2018.06.004

Blethen, S. L., Boeker, E. A., & Snell, E. E. (1968). Argenine decarboxylase from Escherichia coli. I. Purification and specificity for substrates and coenzyme. *Journal of Biological Chemistry*, *243*(8), 1671–1677. https://doi.org/10.1016/S0021-9258(18)93498-8

Boroujeni, M. B., Dastjerdeh, M. S., Shokrgozar, M., Rahimi, H., & Omidinia, E. (2021). Computational driven molecular dynamics simulation of keratinocyte growth factor behavior at different pH conditions. *Informatics in Medicine Unlocked*, *23*, 100514. https://doi.org/10.1016/j.imu.2021.100514

Cava, F., Hidalgo, A., & Berenguer, J. (2009). Thermus thermophilus as biological model. *Extremophiles: Life under Extreme Conditions*, *13*(2), 213–231. https://doi.org/10.1007/s00792-009-0226-6

Colovos, C., & Yeates, T. O. (1993). Verification of protein structures: Patterns of nonbonded atomic interactions. *Protein Science: A Publication of the Protein Society*, *2*(9), 1511–1519. https://doi.org/10.1002/pro.5560020916

Eisenberg, D., Lüthy, R., & Bowie, J. U. (1997). Verify3d: Assessment of protein models with three-dimensional profiles. *Methods in Enzymology*, *277*, 396–404. https://doi.org/10.1016/s0076-6879(97)77022-8

Friedrich, A., Hartsch, T., & Averhoff, B. (2001). Natural transformation in mesophilic and thermophilic bacteria: Identification and characterization of novel, closely related competence genes in Acinetobacter sp. Strain BD413 and Thermus thermophilus HB27. *Applied and Environmental Microbiology*, *67*(7), 3140–3148. https://doi.org/10.1128/AEM.67.7.3140-3148.2001

Forouhar, F., Lew, S., Seetharaman, J., Xiao, R., Acton, T. B., Montelione, G. T., & Tong, L. (2010). Structures of bacterial biosynthetic arginine decarboxylases. *Acta Crystallographica. Section F, Structural Biology and Crystallization Communications*, *66*(Pt 12), 1562–1566. https://doi.org/10.1107/S1744309110040649

Gevrekci, A. Ö. (2017). The roles of polyamines in microorganisms. *World Journal of Microbiology and Biotechnology*, *33*(11), 204. https://doi.org/10.1007/s11274-017-2370-y

Henne, A., Brüggemann, H., Raasch, C., Wiezer, A., Hartsch, T. [., Liesegang, H., Johann, A., Lienard, T., Gohl, O., Martinez-Arias, R., Jacobi, C., Starkuviene, V., Schlenczeck, S., Dencker, S., Huber, R., Klenk, H. -P., Kramer, W., Merkl, R., Gottschalk, G., & Fritz, H. -J. (2004). The genome sequence of the extreme thermophile Thermus thermophilus. *Nature Biotechnology*, *22*(5), 547–553. https://doi.org/10.1038/nbt956

Hofer, S. J., Simon, A. K., Bergmann, M., Eisenberg, T., Kroemer, G., & Madeo, F. (2022). Mechanisms of spermidine-induced autophagy and geroprotection. *Nature Aging*, *2*(12), 1112–1129. https://doi.org/10.1038/s43587-022-00322-9

Hollingsworth, S. A., & Dror, R. O. (2018). Molecular Dynamics Simulation for All. *Neuron*, *99*(6), 1129–1143. https://doi.org/10.1016/j.neuron.2018.08.011

Hori, H. (2019). Regulatory Factors for tRNA Modifications in Extreme-Thermophilic Bacterium Thermus thermophilus. *Frontiers in Genetics*, *10*, 204. https://doi.org/10.3389/fgene.2019.00204

Joyner, J. C., Keuper, K. D., & Cowan, J. A. (2013). Analysis of RNA cleavage by MALDI-TOF mass spectrometry. *Nucleic Acids Research*, *41*(1), e2–e2. https://doi.org/10.1093/nar/gks811

K, D., Kuramitsu, S., Yokoyama, S., Thirumananseri, K., & Ponnuraj, K. (2023). Crystal structure analysis and molecular dynamics simulations of arginase from Thermus thermophilus. *Journal of Biomolecular Structure & Dynamics*, *41*(14), 6811–6821. https://doi.org/10.1080/07391102.2022.2112615

Kawata, M., & Nagashima, U. (2001). Particle mesh Ewald method for three-dimensional systems with two-dimensional periodicity. *Chemical Physics Letters*, *340*(1-2), 165–172. https://doi.org/10.1016/S0009-2614(01)00393-1

Kobayashi, T., Sakamoto, A., Kashiwagi, K., Igarashi, K., Moriya, T., Oshima, T. [., & Terui, Y. (2022). Alkaline Stress Causes Changes in Polyamine Biosynthesis in Thermus thermophilus. *International Journal of Molecular Sciences*, *23*(21), 13523. https://doi.org/10.3390/ijms232113523

Li, J., Abel, R., Zhu, K., Cao, Y., Zhao, S., & Friesner, R. A. (2011). The VSGB 2.0 model: A next generation energy model for high resolution protein structure modeling. *Proteins*, *79*(10), 2794–2812. https://doi.org/10.1002/prot.23106

Lovell, S. C., Davis, I. W., Arendall, W. B., Bakker, P. I. W. D., Word, J. M., Prisant, M. G., Richardson, J. S., & Richardson, D. C. (2003). Structure validation by Calpha geometry: Phi,psi and Cbeta deviation. *Proteins*, *50*(3), 437–450. https://doi.org/10.1002/prot.10286

Morris, D. R., & Pardee, A. B. (1965). A biosynthetic ornithine decarboxylase in Escherichia, coli. *Biochemical and Biophysical Research Communications*, *20*(6), 697–702. https://doi.org/10.1016/0006-291x(65)90072-0

Murray, K. K., Seneviratne, C. A., & Ghorai, S. (2016). High resolution laser mass spectrometry bioimaging. *Methods (San Diego, Calif.)*, *104*, 118–126. https://doi.org/10.1016/j.ymeth.2016.03.002

Narayan, A., & Naganathan, A. N. (2018). Switching Protein Conformational Substates by Protonation and Mutation. *The Journal of Physical Chemistry. B*, *122*(49), 11039–11047. https://doi.org/10.1021/acs.jpcb.8b05108

Ohtani, N., Tomita, M., & Itaya, M. (2010). An extreme thermophile, Thermus thermophilus, is a polyploid bacterium. *Journal of Bacteriology*, *192*(20), 5499–5505. https://doi.org/10.1128/JB.00662-10

Oshima, T. (2007). Unique polyamines produced by an extreme thermophile, Thermus thermophilus. *Amino Acids*, *33*(2), 367–372. https://doi.org/10.1007/s00726-007-0526-z

Oshima, T. (2010). Enigmas of biosyntheses of unusual polyamines in an extreme thermophile, Thermus thermophilus. *Plant Physiology and Biochemistry: PPB*, *48*(7), 521–526. https://doi.org/10.1016/j.plaphy.2010.03.011

Prasher, P., Sharma, M., Singh, S. K., Gulati, M., Chellappan, D. K., Rajput, R., Gupta, G., Ydyrys, A., Kulbayeva, M., Abdull Razis, A. F., Modu, B., Sharifi-Rad, J., & Dua, K. (2023). Spermidine as a promising anticancer agent: Recent advances and newer insights on its molecular mechanisms. *Frontiers in Chemistry*, *11*, 1164477. https://doi.org/10.3389/fchem.2023.1164477

Shukla, R., & Tripathi, T. (2020). Molecular dynamics simulation of protein and protein–ligand complexes. *Computer-Aided Drug Design*, 133–161.

Sievers, F., & Higgins, D. G. (2018). Clustal Omega for making accurate alignments of many protein sequences. *Protein Science: A Publication of the Protein Society*, *XIII*(1), 135–145. https://doi.org/10.1002/pro.3290

Sun, A., Song, W., Qiao, W., Chen, X., Liu, J., Luo, Q., & Liu, L. (2017). Efficient agmatine production using an arginine decarboxylase with substrate-specific activity. *Journal of Chemical Technology & Biotechnology*, *92*(9), 2383–2391. https://doi.org/10.1002/jctb.5245

Tabor, C. W., & Tabor, H. (1984). Polyamines. *Annual Review of Biochemistry*, *53*(1), 749–790. https://doi.org/10.1146/annurev.bi.53.070184.003533

Tabor, C. W., & Tabor, H. (1985). Polyamines in microorganisms. *Microbiological Reviews*, *49*(1), 81–99. https://doi.org/10.1128/mr.49.1.81-99.1985

Takahashi, T., & Kakehi, J. I. (2010). Polyamines: Ubiquitous polycations with unique roles in growth and stress responses. *Annals of Botany*, *105*(1), 1–6. https://doi.org/10.1093/aob/mcp259

Tamakoshi, M., & Oshima, T. (2011). Genetics of Thermophiles. In K. Horikoshi (Ed.), *Extremophiles Handbook.* (pp. 547–566). Springer Japan. https://doi.org/10.1007/978-4-431-53898-1_25

Teh, B. S., Abdul Rahman, A. Y., Saito, J. A., Hou, S., & Alam, M. (2012). Complete genome sequence of the thermophilic bacterium Thermus sp. Strain CCB_US3_UF1. *Journal of Bacteriology*, *194*(5), 1240–1240. https://doi.org/10.1128/JB.06589-11

Terui, Y., Ohnuma, M., Hiraga, K., Kawashima, E., & Oshima, T. (2005). Stabilization of nucleic acids by unusual polyamines produced by an extreme thermophile, Thermus thermophilus. *The Biochemical Journal*, *388*(Pt 2), 427–433. https://doi.org/10.1042/BJ20041778

Thiede, B., Höhenwarter, W., Krah, A., Mattow, J., Schmid, M., Schmidt, F., & Jungblut, P. R. (2005). Peptide mass fingerprinting. *Methods (San Diego, Calif.)*, *35*(3), 237–247. https://doi.org/10.1016/j.ymeth.2004.08.015

UniProt Consortium (2007). The Universal Protein Resource (UniProt). *Nucleic Acids Research*, *35*(Database issue), D193–7. https://doi.org/10.1093/nar/gkl929

Uzawa, T., Hamasaki, N., & Oshima, T. (1993). Effects of novel polyamines on cell-free polypeptide synthesis catalyzed by Thermus thermophilus HB8 extract. *Journal of Biochemistry*, *114*(4), 478–486. https://doi.org/10.1093/oxfordjournals.jbchem.a124203.]

Webb, B., & Sali, A. (2016). Comparative Protein Structure Modeling Using MODELLER. *Current Protocols in Bioinformatics*, *54*(1), 5.6.1–5.6.37. https://doi.org/10.1002/cpbi.3

Wiederstein, M., & Sippl, M. J. (2007). Prosa-web: Interactive web service for the recognition of errors in three-dimensional structures of proteins. *Nucleic Acids Research*, *35*(Web Server issue)issue, W407–10. https://doi.org/10.1093/nar/gkm290

Wu, H. Y., Chen, S. F., Hsieh, J. Y., Chou, F., Wang, Y. H., Lin, W. T., Lee, P. Y., Yu, Y. J., Lin, L. Y., Lin, T. S., Lin, C. L., Liu, G. Y., Tzeng, S. R., Hung, H. C., & Chan, N. L. (2015). Structural basis of antizyme-mediated regulation of polyamine homeostasis. *Proceedings of the National Academy of Sciences of the United States of America*, *112*(36), 11229–11234. https://doi.org/10.1073/pnas.1508187112